

# Incorporating expression data in metabolic modeling: a case study of lactate dehydrogenase

Joshua Downer<sup>†</sup>, Joel R. Sevinsky\*, Natalie G. Ahn\*, Katheryn A. Resing\*, M. D. Betterton<sup>†</sup>

<sup>†</sup>Department of Applied Mathematics, University of Colorado at Boulder, 526 UCB, CO 80309-0526, USA, and

\*Department of Chemistry and Biochemistry, University of Colorado at Boulder, 215 UCB, CO 80309-0215, U.S.A.

Address correspondence to: M. D. Betterton, University of Colorado at Boulder, Department of Applied Mathematics, 526 UCB, CO 80309-0526, U.S.A., Email: mdb@colorado.edu, Phone: 303-735-6135.

## Abstract

Integrating biological information from different sources to understand cellular processes is an important problem in systems biology. We use data from mRNA expression arrays and chemical kinetics to formulate a metabolic model relevant to K562 erythroleukemia cells. MAP kinase pathway activation alters the expression of metabolic enzymes in K562 cells. Our array data show changes in expression of lactate dehydrogenase (LDH) isoforms after treatment with phorbol 12-myristate 13-acetate (PMA), which activates MAP kinase signaling. We model the change in lactate production which occurs when the MAP kinase pathway is activated, using a non-equilibrium, chemical-kinetic model of homolactic fermentation. In particular, we examine the role of LDH isoforms, which catalyze the conversion of pyruvate to lactate. Changes in the isoform ratio are not the primary determinant of the production of lactate. Rather, the total concentration of LDH controls the lactate concentration.

## Keywords

metabolic modeling, MAP kinase, cell signaling, enzyme kinetics, expression data, lactate dehydrogenase

## Introduction

Modeling of cellular metabolism has a long history of important contributions to biology. Approaches include kinetic modeling, metabolic control analysis, flux balance analysis, and metabolic network analysis (Stephanopoulos *et al.*, 1998). A new era of research in metabolism is now possible, because large-scale expression studies can determine levels of many metabolites (Goodacre *et al.*, 2004; Fan *et al.*, 2004) and metabolic enzymes (Ferea *et al.*, 1999; Kal *et al.*, 1999). In this paper we use metabolic enzyme expression data to guide metabolic modeling, with a focus on small but significant changes in mRNA abundance. Our goal is to understand how biologically realistic changes in mRNA abundance of metabolic enzymes affect cellular metabolism. Previous work integrating expression data with metabolic modeling has been done in yeast (Akesson *et al.*, 2004), but not, to our knowledge, in mammalian systems.

We focus on glycolysis, an essential ATP-producing metabolic pathway. The initial reactions of glycolysis break down glucose into pyruvate. Pyruvate can feed into either the citric acid cycle (aerobic metabolism) or homolactic fermentation (anaerobic metabolism) (Voet & Voet, 2004). The reactions involving pyruvate therefore control this important metabolic branch point. Homolactic fermentation is catalyzed by lactate dehydrogenase (LDH) in a compulsory-order, ternary reaction (Borgmann *et al.*, 1975). LDH reversibly converts pyruvate and NADH into lactate and NAD<sup>+</sup>. The isozymes of LDH are tetramers formed from two types of monomers (a third isoform is usually germ-line specific, but can be expressed in cancers (Koslowski *et al.*, 2002)). The two isoforms are labeled H (heart) and M (muscle), and their ratio varies between cell types. The LDH isoform ratio has been proposed to indicate the metabolic state of cells: it is believed that the M isoform favors lactate production while the H isoform favors pyruvate production (Boyer *et al.*, 1963; Stambaugh & Post, 1966; Boyer, 1975; Voet & Voet, 2004). In this framework, the LDH isoform ratio can serve as an indicator of the relative flux through aerobic/anaerobic glycolytic pathways.

Here we use a mathematical model of homolactic fermentation to study the connections between growth-factor signaling and metabolism. It has been known since the work of Warburg that carcinogenesis is accompanied by changes in cellular metabolism (Stubbs *et al.*, 2003; Griffiths *et al.*, 2002; Dang & Semenza, 1999). In particular, tumors typically favor anaerobic metabolism, resulting in higher lactate production relative to non-cancerous cells (Walenta *et al.*, 2004; Newell *et al.*, 1993; Warburg, 1956).

Although inhibition of glycolysis can kill tumor cells (Munoz-Pinedo *et al.*, 2003), the connections between carcinogenesis and metabolic alterations are not fully understood (Fan *et al.*, 2004). However, intriguing connections between metabolic enzymes and cancer have been demonstrated (Kondoh *et al.*, 2005; Kim *et al.*, 2004; Mazurek & Eigenbrodt, 2003). In particular, LDH expression is altered in many tumors (Walenta *et al.*, 2004; Unwin *et al.*, 2003; Maekawa *et al.*, 2003) and cancer cell models (Li *et al.*, 2004; Karan *et al.*, 2002; Lewis *et al.*, 2000). High tumor LDH levels have been shown to correlate with poor prognosis in lung cancer patients (Koukourakis *et al.*, 2003).

In this study, we focus on changes in LDH expression induced by the mitogen-activated protein (MAP) kinase pathway. The MAP kinase cascade is important in cell growth, differentiation, and survival, and alterations of MAP kinase signaling have been found in many cancers (Lewis *et al.*, 1998). The signal is transduced by a series of phosphorylation reactions: MAP kinase proteins phosphorylate and thereby activate their downstream targets. The pathway includes the MAP kinase proteins ERK 1 and 2 and their upstream activators, the MAP kinase kinases MKK 1 and 2. Recent work has found connections between MAP kinase signaling and metabolism. For example, increased expression of LDH-H in human tumors may occur in part because the transcription factor MYC, a downstream target of the MAP kinase pathway, transcriptionally up-regulates the LDH-H gene (Jungmann *et al.*, 1998; Shim *et al.*, 1997). Other genes involved in glycolysis are also affected by MYC (Osthus *et al.*, 2000). Activation of the MAP kinase pathway has been shown to increase LDH activity, glucose uptake, and lactate production (Riera *et al.*, 2003; Papas *et al.*, 1999).

We studied mRNA expression in K562 erythroleukemia cells, a cell line used as a model for leukemia. In our experiments, MAP kinase signaling was either (*i*) activated with phorbol 12-myristate 13-acetate (PMA) or (*ii*) simultaneously activated with PMA and inhibited with U0126, a specific MKK inhibitor. We found small but reproducible changes in the expression of LDH isoforms in response to MAP kinase pathway activation (figure 1), with no significant changes in other enzymes that catalyze reactions involving pyruvate. This result suggests that activating the MAP kinase pathway alters the relative flux through aerobic and anaerobic glycolysis in these cells. We chose to model the expected changes in cellular lactate production to better understand the connections between signaling and metabolism. We hypothesized that the LDH isoform ratio plays an important role in determining cellular lactate levels, as suggested previously (Riera *et al.*, 2003; Dang & Semenza, 1999).

We formulated a chemical-kinetic model of homolactic fermentation based on *in vitro* biochemistry (Borgmann *et al.*, 1975). Our goal was to determine how changes in the LDH isoform ratio alter the amount of lactate produced by K562 cells. We used the experimentally determined abundance changes as model inputs. The model

describes the mass-action kinetics of homolactic fermentation. We included metabolic flux terms in the model to describe the connection between homolactic fermentation and the larger metabolic network of the cell. The metabolic flux is a constant rate of production/consumption of a metabolite through other reactions or transport. Several model inputs—the steady-state concentrations of pyruvate, NADH, and NAD<sup>+</sup>—have not been measured in K562 cells. Therefore we validated our results with a robustness analysis (von Dassow *et al.*, 2000; Barkai & Leibler, 1997).

We present several unexpected findings. In a preliminary analysis, we examined the behavior of each isoform individually. Our results predict that LDH-H produces a larger steady-state lactate concentration than an equivalent amount of LDH-M under typical cellular conditions. This result is surprising because it disagrees with the statement, often found in the literature, that the M isoform favors lactate production while the H isoform favors pyruvate production (Boyer *et al.*, 1963; Stambaugh & Post, 1966; Boyer, 1975; Voet & Voet, 2004). We discuss the reason for this difference and explain why our results are more applicable *in vivo*.

Second, we predict a decrease in the steady-state lactate concentration when the LDH isoform abundance shifts from control to PMA-treated levels. This result means that the H:M isoform ratio alone does not control the lactate concentration. After PMA treatment the ratio of LDH-H to LDH-M changes from 1.02 to 1.35 in our experiments. According to our single-isoform model, an increasing isoform ratio should lead to an *increase* in lactate concentration. This finding led us to consider separately how the isoform ratio and the total abundance of LDH control the lactate concentration. We demonstrate that while the isoform ratio does affect the production of lactate, the experimentally determined total LDH abundance change plays a larger role in determining the lactate concentration.

## Methods

### Cell extraction and microarray analysis

K562 erythroleukemia cells were grown in suspension in 10% FBS/RPMI and treated with 10 nM phorbol 12-myristate 13-acetate (PMA) and 20  $\mu$ M U0126 (Promega) as described previously (Sevinsky *et al.*, 2004). Cells ( $7 \times 10^5$ ) were washed twice in ice cold phosphate buffered saline, 1 mM EDTA, 1 mM EGTA, and total RNA was isolated by TRIzol extraction (Invitrogen). First and second strand cDNA synthesis,

*in vitro* transcription of biotin-labeled cRNA, and fragmentation were carried out following standard protocols from Affymetrix. Probes were hybridized onto U133 2.0 Plus GeneChips (Affymetrix) and processed at the UCHSC Cancer Center Microarray core facility. Datasets were corrected for background and normalized using RMA Express software. Each condition was analyzed in three independent experiments (figure 1).

### Model

We used a chemical-kinetic model to analyze the effect of isoform switching on the non-equilibrium steady state of homolactic fermentation. We assume that the metabolite and enzyme species are homogeneously distributed in the cytosol. This leads to a set of 12 mass-action ordinary differential equations that describe the time evolution of metabolite and enzyme concentrations. Four equations govern the metabolites and four equations govern each of the LDH isoforms and their related complexes (equations 2-4).

Each elementary reaction in the model (figure 2) follows the law of mass action, which results in the following reaction rates

$$v_1 = k_1 x_1 e_1 - k_{-1} e_2, \quad (1a)$$

$$v_2 = k_2 x_2 e_2 - k_{-2} e_3, \quad (1b)$$

$$v_3 = k_3 e_3 - k_{-3} y_1 e_4, \quad (1c)$$

$$v_4 = k_4 e_4 - k_{-4} y_2 e_1, \quad (1d)$$

$$v_5 = k_5 x_1 f_1 - k_{-5} f_2, \quad (1e)$$

$$v_6 = k_6 x_2 f_2 - k_{-6} f_3, \quad (1f)$$

$$v_7 = k_7 f_3 - k_{-7} y_1 f_4, \quad (1g)$$

$$v_8 = k_8 f_4 - k_{-8} y_2 f_1, \quad (1h)$$

where  $x_1$ ,  $x_2$ ,  $y_1$ , and  $y_2$  are the concentrations of NAD<sup>+</sup>, lactate, pyruvate, and NADH;  $e_1$ ,  $e_2$ ,  $e_3$ , and  $e_4$  are the concentrations of LDH-H, LDH-H:NAD<sup>+</sup>, LDH-H:NAD<sup>+</sup>:lactate, and LDH-H:NADH;  $f_1$ ,  $f_2$ ,  $f_3$ , and  $f_4$  are the concentrations of LDH-M, LDH-M:NAD<sup>+</sup>, LDH-M:NAD<sup>+</sup>:lactate, and LDH-M:NADH. The values of the kinetic rate constants are shown in figure 3.

The equations describing the dynamics of the system can be written compactly in terms of the reaction rates. The equations for the metabolites are

$$x_1' = -v_1 - v_5 - \alpha_1, \quad (2a)$$

$$x_2' = -v_2 - v_6 - \alpha_2, \quad (2b)$$

$$y_1' = v_3 + v_7 + \alpha_3, \quad (2c)$$

$$y_2' = v_4 + v_8 + \alpha_4, \quad (2d)$$

where  $\alpha_1$  and  $\alpha_2$  are the flux of NAD+ and lactate out of the system, and  $\alpha_3$  and  $\alpha_4$  are the flux of NADH and pyruvate into the system.

LDH is an efficient catalyst which is thought to operate near equilibrium under many conditions (Borgmann *et al.*, 1975). However, the metabolites in homolactic fermentation are continually consumed or produced in other reactions or transported into and out of the cell. This flux of metabolites means that the system is not in thermodynamic equilibrium. In contrast to an equilibrium system, the steady state of a non-equilibrium reaction depends on the reaction mechanism and the total concentration of the enzyme that catalyzes it. Here we do not specify a mechanism for this metabolic flux but assume that each metabolite is produced or consumed at a constant rate. The constant flux of each metabolite in the model is represented by the constant terms  $\alpha_1, \dots, \alpha_4$  in equation (2).

The heart-isoform complexes obey the equations

$$e'_1 = v_4 - v_1, \tag{3a}$$

$$e'_2 = v_1 - v_2, \tag{3b}$$

$$e'_3 = v_2 - v_3, \tag{3c}$$

$$e'_4 = v_3 - v_4, \tag{3d}$$

and the muscle-isoform complexes obey the equations

$$f'_1 = v_8 - v_5, \tag{4a}$$

$$f'_2 = v_5 - v_6, \tag{4b}$$

$$f'_3 = v_6 - v_7, \tag{4c}$$

$$f'_4 = v_7 - v_8. \tag{4d}$$

We are primarily interested in the steady-state behavior of the model, which occurs only when the fluxes are equal for all four metabolites. In other words, a steady state exists if and only if  $\alpha_1 = \alpha_2 = \alpha_3 = \alpha_4 = \alpha$ , where  $\alpha$  is the constant metabolic flux of the model.

## Numerics

A numerical approach was used to determine the steady-state relationship between the metabolite concentrations, the metabolic flux, and the isoform concentrations with both isoforms present (figure 4). Equations (2)–(4) can be integrated numerically, allowing the system to approach a steady state from any initial condition. However, we specified the steady-state concentrations of NAD+, NADH, and pyruvate, and

determined the corresponding steady-state concentration of lactate (equations (2a), (2c), and (2d) were eliminated from the model).

The differential equations were integrated using a Runge-Kutta-Fehlberg fifth-order method with adaptive stepping (Press *et al.*, 1992). Newton’s method was used to accelerate convergence to the steady state. If the solution to the constrained differential equations was close to a steady state, Newton’s method quickly converged to it (Press *et al.*, 1992). If Newton’s method started too far from the steady state it rapidly diverged. When this happened, the constrained equations were integrated again (continuing from the last solution) for a specified time interval. Integrating for a longer time allowed the system to approach closer to the steady state before Newton’s method was tried again. This hybrid approach worked well for all the conditions we studied.

We note that Newton’s method does not follow the dynamics of the system and does not find the correct steady state unless the equations are additionally constrained. In particular, it is necessary to explicitly enforce the conservation of the total enzyme concentrations (see below).

## Results

### Single-isoform results

We examined the steady-state production of lactate by a single LDH isoform. Under typical cellular conditions our model predicts that LDH-H produces more lactate than LDH-M. This result is surprising because many authors state that LDH-M produces lactate more efficiently than LDH-H (Boyer *et al.*, 1963; Stambaugh & Post, 1966; Boyer, 1975; Voet & Voet, 2004). We explain the reason for this difference, which results from different model assumptions, and argue that our analysis is more experimentally relevant.

#### *Steady-state lactate production by a single isoform*

Here we are interested in the behavior of the model at steady state. All concentrations are assumed to be steady-state values unless otherwise stated. Suppose that the concentrations of pyruvate, NAD<sup>+</sup>, and NADH are known. Furthermore, suppose only one isoform of LDH is present and its total concentration is known. We can then derive an equation that describes the concentration of lactate as a function of the metabolic flux  $\alpha$ . Recall that when  $\alpha > 0$  lactate and NAD<sup>+</sup> are removed from the system and pyruvate and NADH are added to the system.

The total concentration of either enzyme isoform is constant. This can be shown for LDH-H by adding equations (3a)–(3d),

$$e'_1 + e'_2 + e'_3 + e'_4 = 0, \quad (5)$$

and integrating to obtain

$$e_1 + e_2 + e_3 + e_4 = e_0. \quad (6)$$

Here  $e_0$  is the total concentration of the heart isoform. This relation always holds and is not particular to the steady state. The same analysis applies to the muscle isoform:

$$f_1 + f_2 + f_3 + f_4 = f_0, \quad (7)$$

where  $f_0$  is the total concentration of the muscle isoform.

At steady state the rates of change of all variables are zero, so the derivatives in equations (2a)–(2d) are zero. This implies that  $v_1 = v_2 = v_3 = v_4 = -\alpha$ . There are five unknown quantities in the model: the four reaction intermediates involving LDH-H,  $e_1$ ,  $e_2$ ,  $e_3$ , and  $e_4$ , and the lactate concentration,  $x_2$ . (The other metabolite concentrations and the metabolic flux are assumed known). The five equations required for a unique solution are provided by the heart isoform conservation law and the definitions of the reaction rates:

$$e_1 + e_2 + e_3 + e_4 = e_0, \quad (8a)$$

$$k_1 x_1 e_1 - k_{-1} e_2 = -\alpha, \quad (8b)$$

$$k_2 x_2 e_2 - k_{-2} e_3 = -\alpha, \quad (8c)$$

$$k_3 e_3 - k_{-3} y_1 e_4 = -\alpha, \quad (8d)$$

$$k_4 e_4 - k_{-4} y_2 e_1 = -\alpha. \quad (8e)$$

Equations (8a), (8b), (8d), and (8e) form a linear system that determines  $e_1$ ,  $e_2$ ,  $e_3$ , and  $e_4$ . The solutions for  $e_2$  and  $e_3$  can then be substituted into (8c) to determine  $x_2$ . The result is

$$x_2 = \frac{a_0 e_0 - a_1 \alpha}{b_0 e_0 + b_1 \alpha}, \quad (9)$$



where

$$\begin{aligned}
a_0 &= k_{-1}k_{-2}k_{-3}k_{-4}y_1y_2, \\
a_1 &= k_{-1}k_{-2}k_4 + k_{-1}k_3k_4 + k_{-2}k_1k_4x_1 + k_1k_3k_4x_1 + k_{-1}k_{-2}k_{-3}y_1 \\
&\quad + k_{-2}k_{-3}k_1x_1y_1 + k_{-1}k_{-2}k_{-4}y_2 + k_{-1}k_{-4}k_3y_2 + k_{-1}k_{-3}k_{-4}y_1y_2 \\
&\quad + k_{-2}k_{-3}k_{-4}y_1y_2, \\
b_0 &= k_1k_2k_3k_4x_1, \\
b_1 &= k_2k_3k_4 + k_1k_2k_3x_1 + k_1k_2k_4x_1 + k_{-3}k_1k_2x_1y_1 + k_{-4}k_2k_3y_2 \\
&\quad + k_{-3}k_{-4}k_2y_1y_2.
\end{aligned}$$

Note that when  $\alpha = 0$  we recover the equilibrium relationship

$$\frac{x_1x_2}{y_1y_2} = \frac{k_{-1}k_{-2}k_{-3}k_{-4}}{k_1k_2k_3k_4} = K_{eq}, \quad (10)$$

where  $K_{eq}$  is the equilibrium constant. In other words, when the metabolic flux is zero the system approaches an equilibrium steady state, which is independent of the total enzyme concentration.

The concentration of lactate is a function of the metabolic flux,  $\alpha$ , as shown in figure 5. When the metabolic flux is positive (lactate is being removed from the system) LDH-H produces a higher steady-state lactate concentration than an equal concentration of LDH-M. In our calculations we assumed concentrations of NADH, NAD<sup>+</sup>, and pyruvate equal to 0.97  $\mu\text{M}$ , 0.5 mM, and 99.4  $\mu\text{M}$  respectively. However, this qualitative trend—higher steady-state lactate concentration produced by LDH-H—remains unchanged as long as the pyruvate concentration lies between 40  $\mu\text{M}$  and 2 mM. Outside of this range the steady-state solution is infeasible (at steady state one or more of the metabolites has a concentration less than zero) or LDH-M produces more lactate than LDH-H. This interval was found by varying NADH and NAD<sup>+</sup> independently over a wide range of concentrations (0.1  $\mu\text{M}$ – 10.0 mM). Previous measurements of cellular pyruvate concentration have found a range 0.08 – 0.3 mM, although the concentration of pyruvate has been found as high as 0.7 mM in skeletal muscle under tetanic conditions (Stambaugh & Post, 1966; Boyer, 1975; Tilton *et al.*, 1991; Lambeth & Kushmerick, 2002). Therefore, we predict that in most cells LDH-H produces a higher steady-state lactate concentration than an equal amount of LDH-M.

Our result implies that LDH-H produces a greater concentration of lactate in the cell than LDH-M does when the metabolic flux is positive. Previous work on the kinetics of homolactic fermentation has arrived at the opposite conclusion. The difference between our work and previous studies (Stambaugh & Post, 1966) is that we have

focused on the steady state of the reaction. Previous analyses have adopted a Michaelis-Menten approach, examining the behavior of the reaction far from steady state and under *in vitro* conditions. In Michaelis-Menten theory the only possible steady state is the equilibrium state. Our model includes equilibrium as a special case when the metabolic flux is zero (see figure 5). However, when the metabolic flux is nonzero the concentrations of the enzymes and the reaction mechanism contribute to determining the steady state. Thus at steady state LDH-H results in more lactate than LDH-M does when the metabolic flux is positive. This relationship is reversed when the metabolic flux is negative.

### **Predicted change in lactate concentration after MAP kinase activation**

Here we predict how activating the MAP kinase pathway affects the steady-state lactate concentration. Treating K562 cells with PMA activates the MAP kinase pathway. Conversely, U0126 is a downstream inhibitor of MAP kinase signaling which acts on MKK1 and MKK2 (Gross *et al.*, 2000). The array data show changes in the expression of both LDH isoforms after activation of the MAP kinase pathway (figure 1). We used the relative abundances from our array data to model three conditions: (*i*) control (cells are untreated), (*ii*) MAP kinase active (PMA treatment), and (*iii*) MAP kinase partially suppressed (PMA+U0126 treatment).

We used the full model (figure 2), with both isoforms present. The array data determined the relative concentration of each LDH isoform. The concentrations of the metabolites and enzymes in homolactic fermentation were not measured in K562 cells. However, metabolite and enzyme concentrations are available for muscle cells and we used these data as reference values in our model. K562 cells are unlikely to have an identical metabolic state to muscle cells, so we performed a robustness analysis to determine how our results depend on the reference concentrations used. Metabolite concentrations were sampled over two orders of magnitude about the reference values. We verified that our results remain qualitatively unchanged over this range. We used a total LDH concentration of  $3.43 \mu\text{M}$  (Mulquiney & Kuchel, 2003) in the control condition and assumed that the mRNA expression data directly predict protein concentrations. Therefore, in the control model the total concentrations of LDH-H and LDH-M were  $1.98 \mu\text{M}$  and  $1.45 \mu\text{M}$ . For the PMA-treatment condition, the total concentrations of LDH-H and LDH-M were  $1.83 \mu\text{M}$  and  $0.90 \mu\text{M}$ , while for the PMA+U0126-treatment condition, the total concentrations of LDH-H and LDH-M were  $1.27 \mu\text{M}$  and  $1.37 \mu\text{M}$ . The steady-state concentration of lactate was determined numerically as described in Methods, with the steady-state concentrations of  $\text{NAD}^+$ ,  $\text{NADH}$ , and pyruvate set to  $0.5 \text{ mM}$ ,  $0.97 \mu\text{M}$ , and  $99.4 \mu\text{M}$ , respectively, and a metabolic flux of  $10.0 \mu\text{Ms}^{-1}$  (Lambeth & Kushmerick, 2002).

Our model predicts a decrease in lactate concentration for both the PMA and PMA+U0126 conditions (figure 6). The expression data show that activating the MAP kinase pathway with PMA down-regulates LDH-H and LDH-M (figure 1). As a result of these changes, the model predicts a decrease in the cellular lactate level from 37.1  $\mu\text{M}$  to 33.2  $\mu\text{M}$ . Treatment with PMA+U0126 also down-regulates both LDH isoforms (figure 1), leading to a predicted lactate concentration of 33.5  $\mu\text{M}$ .

### *Robustness analysis*

Here we demonstrate the robustness of the model predictions. The experimentally observed changes in LDH-isoform mRNA predict a decrease in lactate concentration after PMA or PMA+U0126 treatment, independent of the precise values of metabolite concentrations used in the model. The values of NADH, NAD+, and pyruvate concentrations can vary among different cell types and growth conditions. While the quantitative predictions depend on the values of the metabolite concentrations, the qualitative result is robust.

We used each metabolite reference value as the mean of a sampled distribution. We chose a lognormal distribution to describe the population of metabolite concentrations because samples vary by large fractional amounts (Boyer, 1975). The standard deviation is one order of magnitude: approximately 68% of the samples are within 0.1–10.0 times the mean concentration. We note that the lognormal distribution is nonnegative, guaranteeing nonnegative concentrations.

We examined  $10^4$  randomly sampled parameter sets (figure 4). For each set of parameters, we calculated the lactate concentration under three conditions: control, treatment with PMA, and treatment with PMA+U0126. Due to our broad sampling of parameter space, we found some parameter sets where the model cannot reach a physically valid steady state (some parameters result in a mathematical steady state with negative lactate concentration). Thus we excluded from our analysis parameter sets that resulted in an invalid steady state for *any* of the three conditions. This exclusion did not significantly alter the lognormal distribution of parameter values (figure 7). We also checked the consistency of the simulations by comparing the distribution of the first 1,000 results with the distribution of the following 9,000 results. There was no statistically significant difference between these two distributions by the Kolmogorov-Smirnov test ( $p < 0.01$ ) (Press *et al.*, 1992).

The median predicted lactate concentration from the randomly sampled parameters (figure 8) follows the same trend observed for the reference parameter set (figure 6). The predicted lactate concentration decreases by 16.9% for the PMA treatment and by 14.8%

for the PMA+U0126 treatment, relative to control. The systematic difference between the three conditions can be seen by comparing sets of simulations corresponding to the same parameter values. The difference histograms (figure 8) show the decrease in lactate concentration from the control to the treated condition.

The predicted lactate levels for the PMA and PMA+U0126 conditions are similar. This result was unexpected because the LDH H:M isoform ratios were different (1.35 for PMA and 0.85 for PMA+U0126). The key difference between the two treatments and the control is the decrease in the total concentration of LDH, an observation that led us to study the effects of isoform switching and abundance changes separately.

### **Isolating the effects of isoform switching and abundance change**

We studied the effects of independently varying the isoform ratio and LDH abundance using the robustness protocol described above (figure 4). First, we obtained concentrations for pyruvate, NAD<sup>+</sup>, and NADH by sampling their distributions. The histograms of sampled values are similar to those shown in figure 7 (data not shown). For each sampled parameter set we performed three simulations: (*i*) control, where the total concentration of LDH was 3.43  $\mu\text{M}$  and the isoform ratio 1.02, (*ii*) increased isoform ratio, where the isoform ratio was 1.35 and the total LDH concentration remained 3.43  $\mu\text{M}$ , and (*iii*) decreased total concentration, where the isoform ratio was the control value (1.02) and the total concentration was 2.47  $\mu\text{M}$ . These values were taken from the mRNA expression data for control and PMA treatment. This analysis allowed us to isolate the effects of changing the isoform ratio and the total concentration of LDH. In each simulation, the steady-state concentration of lactate was determined numerically as described in Methods.

Figure 9 summarizes the effect of increasing the isoform ratio or decreasing the total concentration of LDH. When the isoform ratio is increased, the lactate concentration increases, and when the total concentration is decreased, the lactate concentration decreases. Increasing the isoform ratio increased the lactate concentration for every parameter set sampled. Conversely, decreasing the total concentration consistently decreases the lactate concentration. The effect of decreasing the total concentration is greater than the effect of changing the isoform ratio, given the experimentally observed abundance changes in the isoforms. For these experimental conditions, we predict that the total abundance of LDH is more important than the isoform ratio in determining the lactate concentration.

## **Discussion**

Our mRNA expression data show that activating MAP kinase signaling changes the ratio of lactate dehydrogenase isoforms in K562 cells. We used a mathematical model of lactate production by LDH to calculate the changes in steady-state lactate concentration which result from changes in LDH concentration. We assume that changes in gene expression predict changes in enzyme concentration. We predict that for the experimentally observed changes in LDH, the cellular lactate concentration undergoes a small but significant decrease. The robustness analysis demonstrates that our prediction holds for a wide range of metabolite concentrations. Experiments which measure the lactate concentration in K562 cells under different conditions (control and MAP kinase signaling active) can directly test our prediction.

It is often stated in the literature that the two main LDH isoforms—LDH-H and LDH-M—promote different directions of the homolactic fermentation reaction. The idea that LDH-M favors the production of lactate and LDH-H favors the production of pyruvate is sometimes used to explain experimental results (Baker *et al.*, 1997; Segal & Crawford, 1994). This interpretation of the role of the isoforms was based on *in vitro* biochemistry under Michaelis-Menten conditions, which do not necessarily apply *in vivo*. Homolactic fermentation is influenced by external supply of and demand for the reactants and products, which means the reaction is not isolated. In addition to assuming an isolated reaction, Michaelis-Menten theory describes the behavior of a reaction in its initial stages. However, metabolic reactions in the cell are typically close to steady state.

In our analysis, we focus on the nonequilibrium steady state of the reaction in the presence of a metabolic flux, which represents the production/consumption of NADH, NAD<sup>+</sup>, lactate, and pyruvate by other sources in the cell. Under typical cellular conditions, LDH-H produces a higher steady-state lactate concentration than does LDH-M. We therefore state that LDH-H favors the production of lactate more than LDH-M does. However, this does not imply that LDH-M favors the production of pyruvate. Both isoforms favor the production of lactate when pyruvate is supplied to the reaction (positive metabolic flux). If the metabolic flux is negative, LDH-M produces more lactate than LDH-H.

We show that examining changes in the LDH isoform ratio alone leads to incorrect predictions: changes in total abundance of the isoforms must also be considered. The changes in LDH isoform ratio we observe lead to relatively small predicted changes in the amount of lactate. The changes in total concentration of LDH lead to a larger predicted change in lactate concentration. Taking into account total concentration changes, as well as changes in isoform ratios, is essential for a full understanding of the system.

An important problem in systems biology is the integration of information from

disparate sources (Kitano, 2002). We describe an approach to metabolic modeling that incorporates three important components: (*i*) the use of global profiling data to identify an interesting problem and to guide the quantitative formulation of the model; (*ii*) a kinetic model which describes the full dynamics of the system; and (*iii*) a robustness analysis to support the conclusions. To our knowledge, no previous metabolic modeling work has incorporated all of these elements. The testing of our approach on this small problem is a pilot study for applying the method to larger systems, where the approach can be even more valuable.

In recent years genome-scale profiling has become common. Significant hurdles remain in the interpretation and use of these data: how can information from profiling be integrated to advance our knowledge? In this paper, we began with an intriguing connection found in the experiments: activating MAP kinase signaling changed the expression of LDH isoforms. We predicted changes in cellular lactate metabolism based on the data. The careful analysis of our profiling data allowed us to isolate interesting and new effects. We emphasize that our model is based on experimentally observed changes in LDH expression, so our results are experimentally relevant.

The advantage of using a kinetic model is that we can describe the full dynamics of the system, including time-dependent behavior. Valuable information about dynamics can arise from this approach; for example, the time scale required for the system to reach steady state can be determined. However, use of kinetic models is more complicated than other approaches that do not consider the full dynamics. The major challenge in kinetic modeling is that many parameters are unknown. Therefore, robustness analysis is essential. The robustness analysis demonstrates that our conclusions do not apply only for a specific parameter set, but are true in general. This component of our approach addresses the fundamental problem of unknown parameters in kinetic modeling.

In the future we hope to apply this approach to larger systems. Testing the method on a smaller system (such as the one described in this paper) is an important step in the development of the method. However, we note that our results illustrate the power of carefully analyzing small systems—surprising results can be obtained through studies of this type.

## Acknowledgements

This work was supported by NIGMS project number 1540281. MDB acknowledges support from the Alfred P. Sloan foundation.

## References

- Akesson, M., Forster, J. & Nielsen, J. (2004). Integration of gene expression data into genome-scale metabolic models. *Metabolic Engineering*, **6** (4), 285–293.
- Baker, J. E., Curry, B. D., Olinger, G. N. & Gross, G. J. (1997). Increased tolerance of the chronically hypoxic immature heart to ischemia. *Circulation*, **95**, 1278 – 1285.
- Barkai, N. & Leibler, S. (1997). Robustness in simple biochemical networks. *Nature*, **387** (6636), 913–917.
- Borgmann, U., Laidler, K. J. & Moon, T. W. (1975). Kinetics and thermodynamics of lactate dehydrogenase from beef heart, beef muscle, and flounder muscle. *Canadian Journal of Biochemistry*, **53**, 1196 – 1206.
- Boyer, P. D., ed. (1975). *The Enzymes*, vol. 11., 3rd edition, Academic Press.
- Boyer, P. D., Lardy, H. & Myrbäck, K., eds (1963). *The Enzymes*, vol. 7., 2nd edition, Academic Press.
- Dang, C. V. & Semenza, G. L. (1999). Oncogenic alterations of metabolism. *Trends in Biochemical Sciences*, **24** (2), 68–72.
- Fan, T. W. M., Lane, A. N. & Higashi, R. M. (2004). The promise of metabolomics in cancer molecular therapeutics. *Current Opinion in Molecular Therapeutics*, **6** (6), 584–592.
- Ferea, T. L., Botstein, D., Brown, P. O. & Rosenzweig, R. F. (1999). Systematic changes in gene expression patterns following adaptive evolution in yeast. *Proceedings of the National Academy of Sciences of the United States of America*, **96** (17), 9721–9726.
- Goodacre, R., Vaidyanathan, S., Dunn, W. B., Harrigan, G. G. & Kell, D. B. (2004). Metabolomics by numbers: acquiring and understanding global metabolite data. *Trends in Biotechnology*, **22** (5), 245–252.
- Griffiths, J. R., McSheehy, P. M. J., Robinson, S. P., Troy, H., Chung, Y. L., Leek, R. D., Williams, K. J., Stratford, I. J., Harris, A. L. & Stubbs, M. (2002). Metabolic changes detected by in vivo magnetic resonance studies of hepa-1 wild-type tumors and tumors deficient in hypoxia-inducible factor-1 beta (HIF-1 beta):

- evidence of an anabolic role for the HIF-1 pathway. *Cancer Research*, **62** (3), 688–695.
- Gross, S. D., Schwab, M. S., Taieb, F. E., Lewellyn, A. L., Qian, Y. W. & Maller, J. L. (2000). The critical role of the map kinase pathway in meiosis II in xenopus oocytes is mediated by p90(rsk). *Current Biology*, **10** (8), 430 – 438.
- Jungmann, R. A., Huang, D. L. & Tian, D. (1998). Regulation of LDH-A gene expression by transcriptional and posttranscriptional signal transduction mechanisms. *Journal of Experimental Zoology*, **282** (1-2), 188–195.
- Kal, A. J., van Zonneveld, A. J., Benes, V., van den Berg, M., Koerkamp, M. G., Albermann, K., Strack, N., Ruijter, J. M., Richter, A., Dujon, B., Ansorge, W. & Tabak, H. F. (1999). Dynamics of gene expression revealed by comparison of serial analysis of gene expression transcript profiles from yeast grown on two different carbon sources. *Molecular Biology of the Cell*, **10** (6), 1859–1872.
- Karan, D., Kelly, D. L., Rizzino, A., Lin, M. F. & Batra, S. K. (2002). Expression profile of differentially-regulated genes during progression of androgen-independent growth in human prostate cancer cells. *Carcinogenesis*, **23** (6), 967–975.
- Kim, J. W., Zeller, K. I., Wang, Y., Jegga, A. G., Aronow, B. J., O'Donnell, K. A. & Dang, C. V. (2004). Evaluation of MYC E-box phylogenetic footprints in glycolytic genes by chromatin immunoprecipitation assays. *Molecular and Cellular Biology*, **24** (13), 5923–5936.
- Kitano, H. (2002). Systems biology: a brief overview. *Science*, **295** (5560), 1662 – 1664.
- Kondoh, H., Leonart, M. E., Gil, J., Wang, J., Degan, P., Peters, G., Martinez, D., Carnero, A. & Beach, D. (2005). Glycolytic enzymes can modulate cellular life span. *Cancer Research*, **65** (1), 177–185.
- Koslowski, M., Tureci, O., Bell, C., Krause, P., Lehr, H.-A., Brunner, J., Seitz, G., Nestle, F. O., Huber, C. & Sahin, U. (2002). Multiple splice variants of lactate dehydrogenase C selectively expressed in human cancer. *Cancer Res*, **62** (22), 6750–5.
- Koukourakis, M. I., Giatromanolaki, A., Sivridis, E., Bougioukas, G., Didilis, V., Gatter, K. C. & Harris, A. L. (2003). Lactate dehydrogenase-5 (LDH-5) overexpression



- in non-small-cell lung cancer tissues is linked to tumour hypoxia, angiogenic factor production and poor prognosis. *British Journal of Cancer*, **89** (5), 877–885.
- Lambeth, M. J. & Kushmerick, M. J. (2002). A computational model for glycogenolysis in skeletal muscle. *Ann Biomed Eng*, **30** (6), 808–827.
- Lewis, B. C., Prescott, J. E., Campbell, S. E., Shim, H., Orłowski, R. Z. & Dang, C. V. (2000). Tumor induction by the c-Myc target genes rcl and lactate dehydrogenase A. *Cancer Research*, **60** (21), 6178–6183.
- Lewis, T. S., Shapiro, P. S. & Ahn, N. G. (1998). Signal transduction through MAP kinase cascades. *Advances in Cancer Research, Vol 74*, **74**, 49–139.
- Li, X. R., Qin, C. H., Burghardt, R. & Safe, S. (2004). Hormonal regulation of lactate dehydrogenase-A through activation of protein kinase C pathways in MCF-7 breast cancer cells. *Biochemical and Biophysical Research Communications*, **320** (3), 625–634.
- Maekawa, M., Taniguchi, T., Ishikawa, J., Sugimura, H., Sugano, K. & Kanno, T. (2003). Promoter hypermethylation in cancer silences LDHB, eliminating lactate dehydrogenase isoenzymes 1-4. *Clinical Chemistry*, **49** (9), 1518–1520.
- Mazurek, S. & Eigenbrodt, E. (2003). The tumor metabolome. *Anticancer Research*, **23** (2A), 1149–1154.
- Mulquiney, P. J. & Kuchel, P. W. (2003). *Modeling metabolism with Mathematica*. CRC Press.
- Munoz-Pinedo, C., Ruiz-Ruiz, C., de Almodovar, C. R., Palacios, C. & Lopez-Rivas, A. (2003). Inhibition of glucose metabolism sensitizes tumor cells to death receptor-triggered apoptosis through enhancement of death-inducing signaling complex formation and apical procaspase-8 processing. *Journal of Biological Chemistry*, **278** (15), 12759–12768.
- Newell, K., Franchi, A., Pouyssegur, J. & Tannock, I. (1993). Studies with glycolysis-deficient cells suggest that production of lactic acid is not the only cause of tumor acidity. *Proc Natl Acad Sci U S A*, **90** (3), 1127–31.
- Osthus, R. C., Shim, H., Kim, S., Li, Q., Reddy, R., Mukherjee, M., Xu, Y., Wonsey, D., Lee, L. A. & Dang, C. V. (2000). Accelerated publication - deregulation of glucose transporter 1 and glycolytic gene expression by c-Myc. *Journal of Biological Chemistry*, **275** (29), 21797–21800.

- Papas, K. K., Sun, L., Roos, E. S., Gounarides, J. S., Shapiro, M. & Nalin, C. M. (1999). Change in lactate production in Myc-transformed cells precedes apoptosis and can be inhibited by Bcl-2 overexpression. *Febs Letters*, **446** (2-3), 338–342.
- Press, W. H., Teukolsky, S. A., Vetterling, W. T. & Flannery, B. P. (1992). *Numerical Recipes in Fortran*. Second edition, Cambridge University Press.
- Riera, M. F., Meroni, S. B., Pellizzari, E. H. & Cigorraga, S. B. (2003). Assessment of the roles of mitogen-activated protein kinase and phosphatidyl inositol 3-kinase/protein kinase B pathways in the basic fibroblast growth factor regulation of Sertoli cell function. *Journal of Molecular Endocrinology*, **31** (2), 279–289.
- Segal, J. A. & Crawford, D. L. (1994). LDH-B enzyme expression: the mechanisms of altered gene expression in acclimation and evolutionary adaptation. *Am J Physiol*, **267** (4 Pt 2), R1150–3.
- Sevinsky, J., Whalen, A. & Ahn, N. (2004). Extracellular signal regulated kinase induces the megakaryocyte GPIIb/CD41 gene through MafB/Kreisler. *Mol. Cell. Biol.* **24**, 4534 – 4545.
- Shim, H., Dolde, C., Lewis, B. C., Wu, C. S., Dang, G., Jungmann, R. A., DallaFavera, R. & Dang, C. V. (1997). c-Myc transactivation of LDH-A: Implications for tumor metabolism and growth. *Proceedings of the National Academy of Sciences of the United States of America*, **94** (13), 6658–6663.
- Stambaugh, R. & Post, D. (1966). Substrate and product inhibition of rabbit muscle lactic dehydrogenase heart (H<sub>4</sub>) and muscle (M<sub>4</sub>) isozymes. *Journal of Biological Chemistry*, **241** (7), 1462 – 1467.
- Stephanopoulos, G., Aristidou, A. & Nielsen, J. (1998). *Metabolic engineering: principles and methodologies*. Academic Press, San Diego.
- Stubbs, M., Bashford, C. L. & Griffiths, J. R. (2003). Understanding the tumor metabolic phenotype in the genomic era. *Current Molecular Medicine*, **3** (1), 49–59.
- Tilton, W. M., Seaman, C., Carriero, D. & Piomelli, S. (1991). Regulation of glycolysis in the erythrocyte: role of the lactate/pyruvate and NAD/NADH ratios. *J Lab Clin Med*, **118** (2), 146–52.

- Unwin, R. D., Craven, R. A., Harnden, P., Hanrahan, S., Totty, N., Knowles, M., Eardley, I., Selby, P. J. & Banks, R. E. (2003). Proteomic changes in renal cancer and co-ordinate demonstration of both the glycolytic and mitochondrial aspects of the Warburg effect. *Proteomics*, **3** (8), 1620–1632.
- Voet, D. & Voet, J. (2004). *Biochemistry*. 3rd edition, Wiley and sons.
- von Dassow, G., Meir, E., Munro, E. M. & Odell, G. M. (2000). The segment polarity network is a robust development module. *Nature*, **406** (6792), 188–192.
- Walenta, S., Schroeder, T. & Mueller-Klieser, W. (2004). Lactate in solid malignant tumors: potential basis of a metabolic classification in clinical oncology. *Current Medicinal Chemistry*, **11** (16), 2195–2204.
- Warburg, O. (1956). On the origin of cancer cells. *Science*, **123** (3191), 309–14.

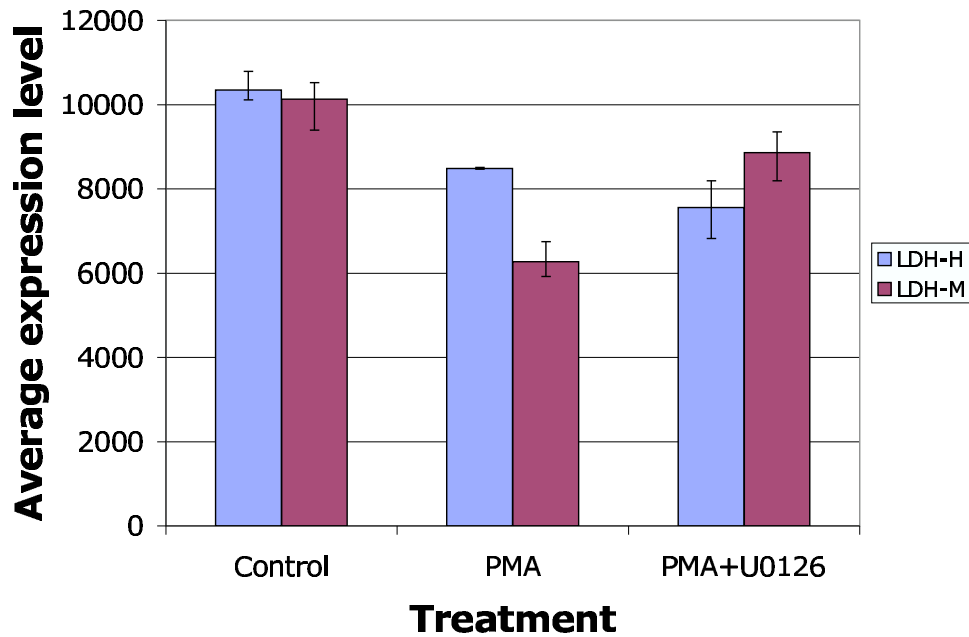


Figure 1: Changes in LDH-H and LDH-M mRNA expression after treatment with PMA and PMA+U0126. PMA treatment activates the MAP kinase pathway, while U0126 is a downstream MAP kinase inhibitor. The data were obtained from experiments performed on Affymetrix gene chips in triplicate (see text). Each data point is the average of three measurements and the error bars represent the maximum and minimum values. Treatment with PMA reduces the abundance of both LDH isoforms, and the M isoform shows a larger reduction. Treatment with PMA+U0126 reduces the abundance of both isoforms (relative to control), but the H isoform shows a larger reduction. The expression levels of LDH-M are significantly different among all of the treatments ( $p < 0.07$ ). The expression levels of LDH-H for the PMA and PMA+U0126 treatments are not significantly different from one another, but they are both significantly different from the expression level of LDH-H in the control ( $p < 0.02$ ).

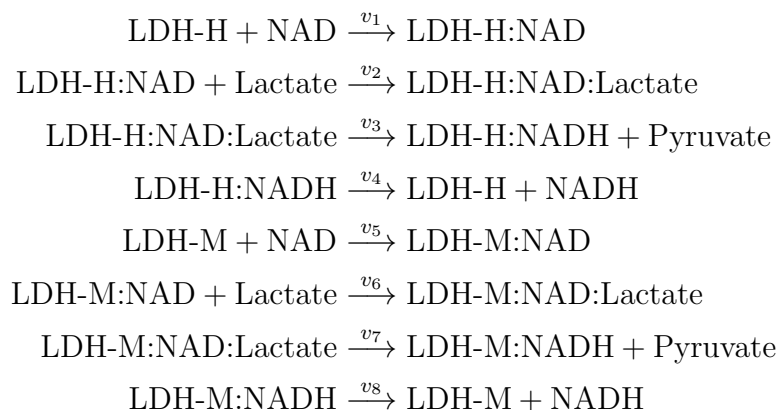


Figure 2: The elementary reactions of homolactic fermentation. Homolactic fermentation is a compulsory-order, ternary reaction. All elementary reactions are reversible. The arrow in each elementary reaction indicates the direction of a positive reaction rate.

$$\begin{array}{ll}
k_1 = 1.45 \times 10^6 \text{ M}^{-1}\text{s}^{-1} & k_{-1} = 1.88 \times 10^3 \text{ s}^{-1} \\
k_2 = 2.06 \times 10^5 \text{ M}^{-1}\text{s}^{-1} & k_{-2} = 1.27 \times 10^3 \text{ s}^{-1} \\
k_3 = 3.29 \times 10^4 \text{ s}^{-1} & k_{-3} = 5.29 \times 10^7 \text{ M}^{-1}\text{s}^{-1} \\
k_4 = 4.33 \times 10^2 \text{ s}^{-1} & k_{-4} = 8.66 \times 10^7 \text{ M}^{-1}\text{s}^{-1} \\
k_5 = 7.50 \times 10^5 \text{ M}^{-1}\text{s}^{-1} & k_{-5} = 3.75 \times 10^2 \text{ s}^{-1} \\
k_6 = 4.10 \times 10^4 \text{ M}^{-1}\text{s}^{-1} & k_{-6} = 1.59 \times 10^3 \text{ s}^{-1} \\
k_7 = 1.51 \times 10^4 \text{ s}^{-1} & k_{-7} = 9.52 \times 10^6 \text{ M}^{-1}\text{s}^{-1} \\
k_8 = 6.65 \times 10^2 \text{ s}^{-1} & k_{-8} = 1.40 \times 10^8 \text{ M}^{-1}\text{s}^{-1}
\end{array}$$

Figure 3: Rate constants in the kinetic model (Borgmann *et al.*, 1975).

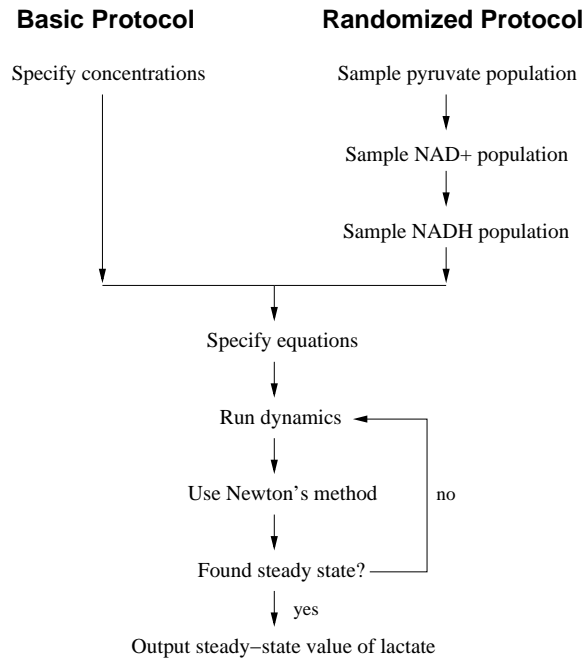


Figure 4: Schematic of the computational protocol. The concentrations of pyruvate, NAD<sup>+</sup>, and NADH are determined in one of two ways: either they are specified (basic protocol) or they are randomly sampled (randomized protocol). The total concentrations of LDH-H and LDH-M are determined from the experimental conditions with both isoforms present. We determine the steady-state concentration of lactate using a hybrid approach. The model will relax to steady state if integrated sufficiently long, but Newton's method accelerates the convergence to steady state.

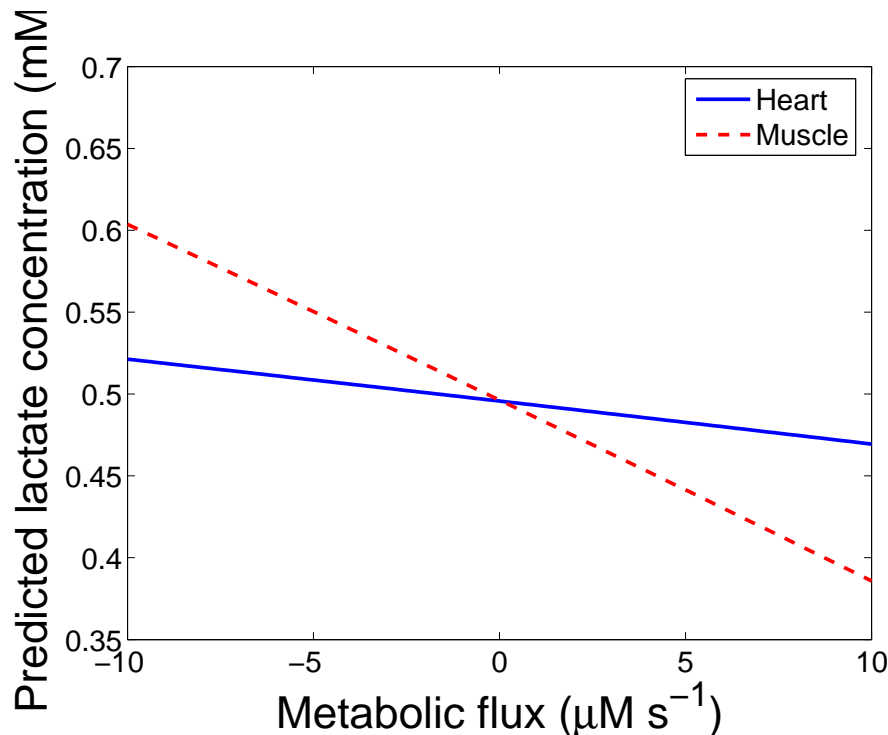


Figure 5: The predicted concentration of lactate as a function of the metabolic flux  $\alpha$ . In the model, a non-equilibrium steady state is possible when pyruvate and NADH are added to the system at a constant rate  $\alpha$ , and lactate and NAD<sup>+</sup> are removed at the same constant rate. These terms in the model represent the production of pyruvate (and consumption of lactate) in other chemical reactions or transport into/out of the cell. As the metabolic flux  $\alpha$  is varied, the steady-state lactate concentration predicted by the model changes. Note that  $\alpha > 0$  means that lactate is being removed from the system. In each of the curves shown, only one of the LDH isoforms is present. The concentrations of the metabolites and the total amount of each enzyme are held constant (pyruvate, 99.4  $\mu\text{M}$ ; NAD<sup>+</sup>, 0.5 mM; NADH, 0.97  $\mu\text{M}$ ; LDH, 3.43  $\mu\text{M}$ ). The sign of the metabolic flux determines which of the two isoforms favors the production of lactate. This conclusion differs from previous analyses of this reaction, which were performed under Michaelis-Menten conditions (see text). The experimental verification of this prediction is future work.

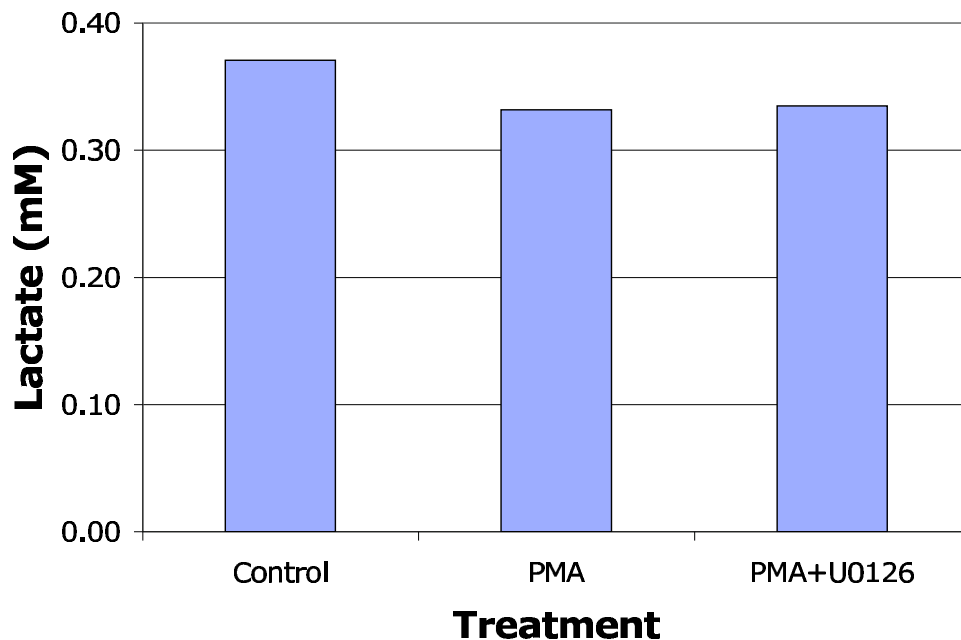


Figure 6: Predicted concentration of lactate for three conditions which simulate control, treatment with PMA, and treatment with PMA+U0126. The three conditions differ in the activity of the MAP kinase pathway. PMA treatment (which activates MAP kinase signaling) results in a small but significant decrease in predicted lactate concentration of 10.5%. Treatment with PMA+U0126 slightly increases the lactate level relative to the PMA treatment. The similar lactate levels for PMA and PMA+U0126 are surprising, because the LDH H:M ratio is 1.35 for the PMA treatment and 0.85 for the PMA+U0126 treatment. The concentrations of pyruvate, NAD<sup>+</sup>, and NADH are 99.4  $\mu\text{M}$ , 0.5 mM, and 0.97  $\mu\text{M}$ . The metabolic flux  $\alpha$  is 10.0  $\mu\text{M s}^{-1}$ .



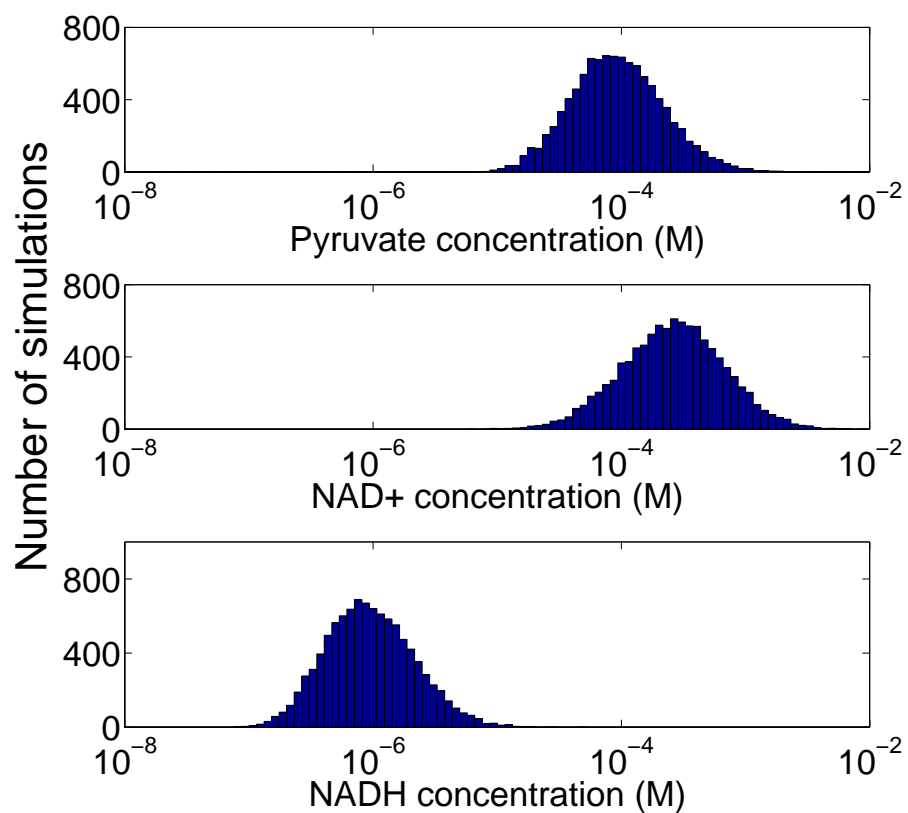


Figure 7: Sampled metabolite concentration values. The distribution of each concentration is lognormal (see text). The mean of each distribution coincides with the reference concentration of that metabolite, and the standard deviation is one order of magnitude.

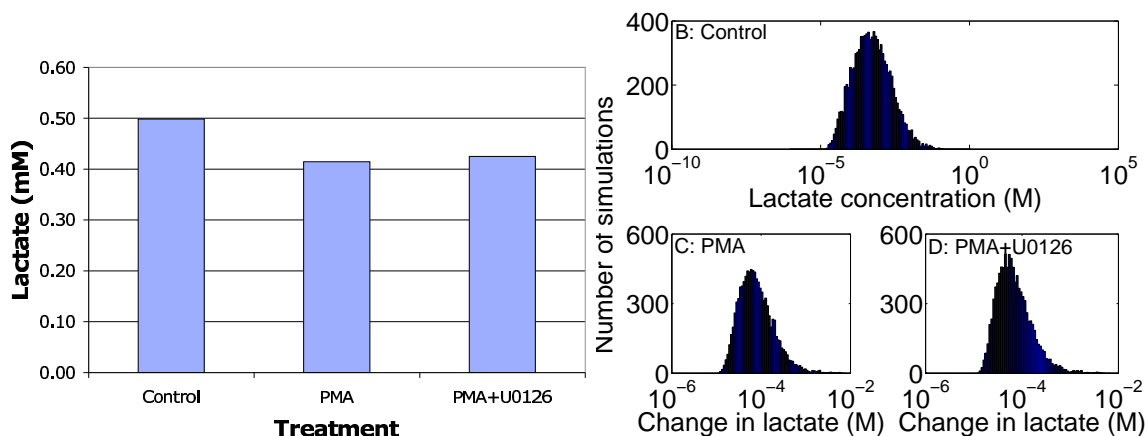


Figure 8: Treating K562 cells with PMA or PMA+U0126 is predicted to result in a similar concentration of lactate. (A) The median concentration of lactate under the three conditions examined in the robustness analysis (control, PMA, and PMA+U0126). This result is qualitatively similar to the result from the simulations using only the reference concentrations of pyruvate, NAD<sup>+</sup>, and NADH (figure 6). Treatment with PMA or PMA+U0126 decreases the concentration of lactate. (B) Histogram of the predicted lactate concentration for the control simulation. This panel illustrates the distribution of the lactate concentration found in the robustness analysis. The median of this histogram is the value of the control treatment shown in A. (C) Histogram of the difference between the lactate concentration predicted for the control and PMA treatment conditions. All of the differences are positive, which means that PMA treatment is predicted to decrease the steady-state lactate concentration. After PMA treatment, the LDH isoform ratio increases from 1.02 to 1.35. (D) Histogram of the difference between the lactate concentration predicted for the control and PMA+U0126 treatment conditions. All of the differences are positive, which means that PMA+U0126 treatment is predicted to decrease the steady-state lactate concentration. After PMA+U0126 treatment, the LDH isoform ratio decreases from 1.02 to 0.85.

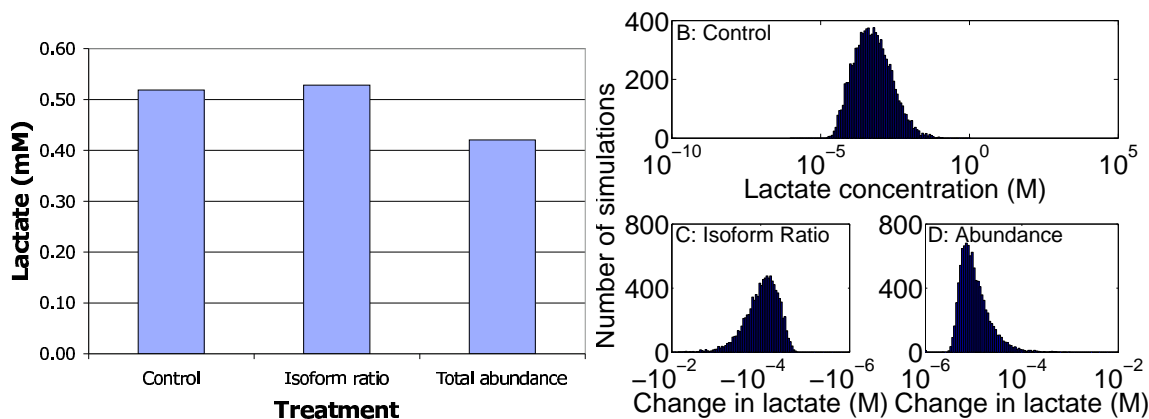


Figure 9: The contrasting effects of increasing the isoform ratio and decreasing the total concentration of LDH. (A) The median concentration of lactate under the three conditions examined (control, isoform-ratio increase, total LDH concentration decrease). When the isoform ratio is increased and the total concentration of LDH is held constant, the amount of lactate produced increases by a small amount. This trend is consistent with the behavior of the individual isoforms: LDH-H produces more lactate than LDH-M for  $\alpha > 0$ . When the isoform ratio is held constant and the total concentration of LDH is reduced, the amount of lactate produced decreases. (B) Histogram of the predicted lactate concentration for the control simulation. This panel illustrates the distribution of the lactate concentration found in the robustness analysis. The median of this histogram is the value of the control treatment shown in A. (C) Histogram of the difference between the lactate concentration predicted for the isoform-ratio increase and control conditions. Every set of metabolites resulted in an increase in the predicted lactate concentration. (D) Histogram of the difference between the lactate concentration predicted for the total LDH concentration decrease and control conditions. Every set of metabolites resulted in a decrease in the predicted lactate concentration. Note that the magnitude of the change in the lactate concentration is approximately 10 times larger than the effect of changing the isoform ratio (shown in C). The influence of the total concentration of LDH on the production of lactate is much greater than the influence of the isoform ratio.